Improving light-based geolocation by including sea surface temperature

Anders Nielsen[*]
Pelagic Fisheries Research Program
Joint Institute for Marine and Atmospheric Research
University of Hawai'i at Manoa
1000 Pope Road, MSB 312, Honolulu, HI, 96822, U.S.A.

Keith A. Bigelow
NOAA/Pacific Islands Fisheries Science Center
2570 Dole St., Honolulu, HI, 96822, U.S.A.

Michael K. Musyl and John R. Sibert
Pelagic Fisheries Research Program
Joint Institute for Marine and Atmospheric Research
University of Hawai'i at Manoa
Honolulu, HI, 96822, U.S.A.

[*]Corresponding author: Anders Nielsen
Fax: (808) 956-4104; email: anders.nielsen@hawaii.edu

20th May 2005

ABSTRACT

An approach to integrate sea surface temperature (SST) measurements into estimates of geolocations calculated by changes in ambient light level from data downloaded from pop-up satellite archival tags (PSAT) is presented. The model is an extension of an approach based on Kalman filter estimation in a state-space model. The approach uses longitude and latitude estimated from light, and SST. The extra information on SST is included in a consistent manner within the milieu of the Kalman filter. The technique was evaluated by attaching PSATs directly on thermistor-equipped GPS drifter buoys. Sea surface temperatures measured in the PSATs and drifter buoy were statistically compared to SSTs determined from satellites. The method is applied to two tracks derived from PSAT tagged blue sharks (*Prionace glauca*) in the central Pacific Ocean. The inclusion of SST in the model produced substantially more probable tracks with lower prediction variance than those estimated from light level data alone.

Keywords: blue shark, geolocation errors, Hawaii, Kalman filter, Lagrangian drifters, pop-up satellite archival tags, sea surface temperature.

INTRODUCTION

Fisheries research organizations, universities, and governments spend large amounts of funding on electronic tagging devices to address a variety of fundamental biological and practical management questions (e.g. Arnold and Dewar 2001; Gunn and Block 2001). Electronic tagging devices are used to gain information about fisheries interactions, post-release survivability, and to delimit spawning locations and migration corridors. As water is (nearly) impenetrable to radio waves, alternative strategies are needed in electronic tagging devices to provide estimates of geographical location (i.e. geolocations) for fishes that do not regularly visit the surface. For animals that breath air, and hence are at the surface for long periods, it is possible to use Argos or GPS tags, which are highly accurate. Archival or data storage tags (DSTs) and pop-up satellite archival tags (PSATs) are electronic tags that store ambient light level data from which estimates of dawn and dusk can be used to calculate longitude (from local noon) and latitude (from local day length) (Musyl et al. 2001; Wilson et al. 1992; Hill 1994).

1

Despite their enormous potential, archival tags and PSATs have several limitations, including tag retention, variable reporting rates, amount of transmitted data and the magnitude and extent of geolocation errors from light-based techniques. This paper provides a method that can be used to improve the accuracy of light-based geolocation estimates so that these may be applied to analyze movement in relation to oceanographic variability.

Raw geolocations (i. e. unfiltered and uncorrected) derived from light-based algorithms are often very noisy, and it is not uncommon that devices are mistakenly 'placed' hundreds of kilometers from their actual location (Musyl et al. 2001; Sibert et al. 2003; Gunn et al. 1994). Estimation of latitude by light-based methods around the time of the equinox can be especially problematic because day length is nearly equal at all latitudes. Light-based geolocation methods are often rendered even more difficult by the behavior of the animals. For instance, animals such as swordfish and bigeye tuna spend a substantial fraction of the day at great depth where light intensity is near the threshold of sensitivity for most electronic tags, or dive near the time of sunrise and sunset (Musyl et al. 2003). It is obvious that these raw geolocations are essentially useless by themselves because of the likely magnitude and extent of geolocation errors.

A widely used (e. g. Musyl et al. 2003; Wilson et al. 2005), and in most cases successful, approach to make sense of these raw geolocations is based on a state-space model (Sibert et al. 2003), and estimated by the Kalman filter (Harvey 1990). This model assumes that the tagged individual moves according to a biased random walk, and the raw geolocations are interpreted as the true position plus some measurement error. The measurement error is parameterized to produce large latitude errors near an equinox and smaller latitude errors near a solstice, which is often seen in the raw geolocations as a side effect of light-based geolocation (Hill and Braun 2001). State-space models are also used in animal tracking in combination with the Bayesian paradigm, where prior beliefs are part of the specified model (Jonsen et al. 2003).

The Kalman filter is named after Rudolph Emil Kalman, who published this elegant recursive method (Kalman 1960). The Kalman filter is one of the most well-known and often-used tools in statistical time series analysis, with a wealth applications in for instance finance, missile guidance, and interactive computer graphics. The usages of the Kalman filter is described in full details in the methods section, but intuitively this approach uses two components: raw geolocations; and predictions from the underlying random walk. The method uses the raw geolocations to estimate the random walk parameters in the periods when data are reliable, but relies mainly on the random walk predictions in periods where data are unreliable.

However, most electronic tagging devices store more than just light intensities. Water temperature and pressure (depth) are also commonly stored. Ancillary information can be used to estimate geographic position. In particular, Smith and Goodman (1986) envisaged the use of ambient water temperature to estimate latitude. The use of SST to estimate latitude from archival tags has since become common (e.g. Inagake et al. 2001, Takahashi et al. 2003, Teo et al. 2004)

The data stored in electronic tags represent a substantial investment of time and financial resources. Temperature measurements are already stored in the tags, and using them to refine the geolocation estimates from the tags is a logical extension. The purpose of this paper is to extend a model relying only on raw geolocations to a model that also uses all the information available from the tags — longitude, latitude and SST. The method developed in this paper is not restricted to SST, but could potentially be used to reconstruct tracks from other measurements (e.g. depth and temperature at depth) if they were available.

MATERIALS AND METHODS

Wildlife Computers pop-up archival transmitting tags (PAT, version 2) were deployed on two WOCE/GPS drifter buoys (ClearSat-15 from Clearwater Instrumentation, Inc.), and set to pop up after nine months. The tags were attached with short monofilament tethers (ca. 40 cm) so that they would float at the surface without being shaded by the bouys for extended periods. Both drifter buoys were deployed (PAT 21760 at (161.9748W,23.08595N) and PAT 21765 at (174.5375W,26.3036N)) in September 2002 prior to the equinox and set to acquire hourly histograms of depth and temperature.

As part of ongoing investigations to determine post-release survivability in blue shark (*Prionace glauca*) released from longline fishing gear, model PTT-100 PSATs from Microwave Telemetry (MT) were affixed to 2 blue sharks in the central Pacific Ocean (Musyl and Brill, unpublished results). In these studies, sharks were caught by conventional longline fishing gear configured in typical Hawaiian "swordfish" style (i.e. shallow nighttime sets (ca. less than 100m as determined by attached Time Depth Recorders (TDRs), about 4-5 hooks per basket with a green chemical light stick above each dropper usually baited with squid (*Illex spp.*) on 15/0 hooks). Sharks were brought on board the NOAA research vessel *Townsend Cromwell* in a sling and were restrained by crew with mattresses. PSATs were affixed to shark's dorsal fin by

3

drilling a hole (ca. 10-15mm diameter) near the base of the fin and threading 49 braid stainless steel wire encased in Tygon tubing which acted as the harness. Stainless crimps were used to attach the harness to a tether made of 122kg fluorocarbon which was crimped to the nosecone of the PSAT.

PSATs from MT deployed on sharks were programmed to acquire raw temperature and pressure (depth) readings every hour and the tag's pop-off dates were set at 13 months after deployment. "Fail-safe" options were programmed in the PSAT to receive data in the event the animal died and sank or if the tag was shed. In the event of a sinking PSAT, a pressure release mechanism (corrosional link) was set at 1200 m. In this scenario, the tag jettisons from the shark and floats to the surface to start transmitting data to ARGOS satellites. Alternatively, if the tag doesn't experience any significant pressure changes in four consecutive days (e.g. shed tag floating at the surface or a stationary tag at a depth less than 1200m), it will automatically initiate data recovery procedures. For the MT tags, estimates for dawn and dusk are automatically calculated in the tag by a proprietary algorithm (Gunn and Block 2001). PSAT 13097 was affixed to an approximately 2m female blue shark on 2 April 2001 at (158.76W, 28.28N), and PSAT 13093 was affixed to 1.5m female blue shark on 11 April 2001 at (158.28W, 18.88N).

Two satellite-derived SST products were obtained for inclusion in the Kalman filter. Fine-scale SST fields (error estimate 0.3–0.5°C) at a resolution of 9 km and 8-day averages were obtained from AVHRR (Advanced Very High Resolution Radiometers) Pathfinder data (Vazquez et al. 1998). Mesoscale SST fields (error estimate 0.7°C) at geographic resolution of 1° and a weekly time-scale were based on an optimal interpolation analysis of AVHRR and *in situ* ship and buoy data (Reynolds and Smith 1994). Fine-scale data were used for the blue shark tags. Mesoscale data were used for the drifter buoy tags as these data have no gaps caused by clouds. The rationale for using the mesoscale product was to simplify the computations, because the geolocation estimates for the buoys were so poor.

Model

The model is based on an improved and extended version of the state-space Kalman filter model of Sibert et al. (2003), where the state equation is describing the movements along the sphere. A random walk model is assumed:

(1)
$$\alpha_i = \alpha_{i-1} + c_i + \eta_i, \quad i = 1, \ldots, T$$

Here α_i is a two dimensional vector containing the coordinates $(\alpha_{i,1}, \alpha_{i,2})$ in nautical miles along the sphere from longitude=0 and latitude=0 at time t_i, c_i is the drift vector describing the deterministic part of the movement, and η_i is the noise vector describing the random part of the movement. The deterministic part of the movement is assumed to be proportional to time $c_i = (u\Delta t_i, v\Delta t_i)'$. The random part is assumed to be serially uncorrelated and follow a two dimensional Gaussian distribution with mean vector 0 and covariance matrix $Q_i = 2D\Delta t_i I_{2\times 2}$.

The measurement equation of the state-space model is a nonlinear function describing the expected observation at a given state (α_i). Each observation y_i consists of three elements: longitude, latitude, and SST. The first two coordinates are the light-based geolocation estimates and the last is the SST recorded by the tag. The measurement equation describing y_i is:

$$(2) \qquad y_i = z(\alpha_i) + d_i + \varepsilon_i, \quad i = 1,\ldots,T$$

The first two coordinates of z comprise the coordinate change function, and the last coordinate describes the expected SST at a given position. z is given by:

$$(3) \qquad z(\alpha_i) = \begin{pmatrix} \frac{\alpha_{i,1}}{60\cos(\alpha_{i,2}\pi/180/60)} \\ \frac{\alpha_{i,2}}{60} \\ \tau\left(\frac{\alpha_{i,1}}{60\cos(\alpha_{i,2}\pi/180/60)}, \frac{\alpha_{i,2}}{60}\right) \end{pmatrix}$$

Here the factor $\pi/180$ converts from degrees to radians, and 60 is the distance corresponding to one degree of longitude at the equator. The function $\tau(\text{longitude}, \text{latitude})$ describes the expected SST at a given location and time. How this function is constructed will be described later. The observational bias $d_i = (b_{\text{lon}}, b_{\text{lat}}, b_{\text{sst}})'$, if present, describes systematic measurement errors, for instance if the internal clock in the tag is not absolutely correct. The bias term was not necessary in any of the tracks presented in this paper. The measurement error ε_i is assumed to follow a Gaussian distribution with mean vector 0 and covariance matrix H_i, where

$$(4) \qquad H_i = \begin{pmatrix} \sigma^2_{\text{lon}} & 0 & 0 \\ 0 & \sigma^2_{\text{lat}_i} & 0 \\ 0 & 0 & \sigma^2_{\text{sst}} \end{pmatrix}$$

5

The variance of the latitude measurements $\sigma^2_{\text{lat}_i}$ is closely related to the equinox, as measurements close to an equinox have large latitude errors. The following variance structure is assumed:

$$(5) \qquad \sigma^2_{\text{lat}_i} = \frac{\sigma^2_{\text{lat}_0}}{\cos^2(2\pi(J_i + (-1)^{s_i} b_0)/365.25) + a_0}$$

where J_i is the number of days since last solstice prior to all observations, s_i is the season number since the beginning of the track (one as long as $J_i < 182.625$, then two for the next 182.625 days, then three and so on). The model parameter b_0 express the number of days, before or after alternating with season, the latitude errors will peak compared to the date of the equinox. The model parameter $\sigma^2_{\text{lat}_0}$ is the minimum latitude variance, and a_0 ensures an upper bound for the latitude variance.

Extended Kalman filter

As the model described in the previous section is non-linear, an approximation is needed to apply the Kalman filter. The extended Kalman filter (Harvey 1990) simply uses a first order Taylor approximation around the optimal estimator $\widehat{\alpha}_{i|i-1}$:

$$(6) \qquad z(\alpha_i) \approx z(\widehat{\alpha}_{i|i-1}) + \widehat{Z}_i\,(\alpha_i - \widehat{\alpha}_{i|i-1})$$

Here $\widehat{Z}_i$ is the first derivative (or the Jacobi matrix) of the function z, which is calculated as:

$$(7) \quad z'(\alpha_i) = \frac{\partial z(\alpha_i)}{\partial \alpha_i} = \begin{pmatrix} \dfrac{1}{60\cos(\alpha_{i,2}\cdot\pi/180/60)} & \dfrac{\alpha_{i,1}\pi\sin(\alpha_{i,2}\cdot\pi/180/60)}{180(60\cos(\alpha_{i,2}\cdot\pi/180/60))^2} \\[2ex] 0 & \dfrac{1}{60} \\[2ex] \dfrac{\partial\tau}{\partial z_{i,1}}\dfrac{1}{60\cos(\alpha_{i,2}\cdot\pi/180/60)} & \dfrac{\partial\tau}{\partial z_{i,1}}\dfrac{\alpha_{i,1}\pi\sin(\alpha_{i,2}\cdot\pi/180/60)}{180(60\cos(\alpha_{i,2}\cdot\pi/180/60))^2} + \dfrac{\partial\tau}{\partial z_{i,2}}\dfrac{1}{60} \end{pmatrix}$$

The optimal estimator $\widehat{\alpha}_{i|i-1}$ is inserted into the matrix in (7) to obtain $\widehat{Z}_i$. The extended Kalman filter update equations are written as:

(8) $\quad \widehat{\alpha}_{i|i-1} = \widehat{\alpha}_{i-1} + c_i$ $\qquad\qquad\qquad$ predict next position

(9) $\quad P_{i|i-1} = P_{i-1} + Q_i$ $\qquad\qquad\qquad$ calculate its variance

(10) $\quad F_i = \widehat{Z}_i P_{i|i-1} \widehat{Z}_i' + H_i$ $\qquad\qquad$ transform into measurement variance

(11) $\quad w_i = y_i - z(\widehat{\alpha}_{i|i-1}) - d_i$ $\qquad\quad$ calculate prediction error

(12) $\quad \widehat{\alpha}_i = \widehat{\alpha}_{i|i-1} + P_{i|i-1} \widehat{Z}_i' F_i^{-1} w_i$ $\qquad$ adjust prediction with observation

(13) $\quad P_i = P_{i|i-1} - P_{i|i-1} \widehat{Z}_i' F_i^{-1} \widehat{Z}_i P_{i|i-1}$ $\quad$ adjust prediction variance

The filter is started by calculating $\widehat{\alpha}_0 = z^{-1}(y_0)$ and assuming this position to be known without error ($P_0 = 0_{2\times 2}$).

Model parameters are estimated by maximum likelihood; the negative log-likelihood function for the Kalman filter is (Harvey 1990):

$$(14) \qquad \ell(\theta) = -\log L(Y|\theta) = \frac{3T}{2} \log(2\pi) + 0.5 \sum_{i=1}^{T} \log(|F_i|) + 0.5 \sum_{i=1}^{T} w_i' F_i^{-1} w_i.$$

Obtaining the sea surface temperature field τ and its derivative

The temperature field τ and its derivatives $\frac{\partial \tau}{\partial z_{i,1}}$ and $\frac{\partial \tau}{\partial z_{i,2}}$ must be known in order to evaluate the coordinate change function (3). Naturally the temperature field is not known, but must be estimated from observations. A fine-scale SST field is comprised of approximately 200,000 measurements. Such a substantial volume of data could probably be handled directly in the Kalman filter numerical optimization, but would require a substantial amount of computer memory (or some pretty clever data structures).

Smoothing of observed SST field is appropriate for this work for several reasons. The Kalman filter requires that τ and its derivatives be evaluated at all points within the study area. Observations are often missing in some areas due to cloud cover. The observed SST field may be very irregular so that the apparent SST may vary substantially over short distances due to fine structure in the temperature field or to measurement noise. Finally, the daily SST estimate computed from the data recorded by the tag is in fact a daily average, so even if the true SST field is not smooth, the tag measurement corresponds to a field with has been locally smoothed by averaging.
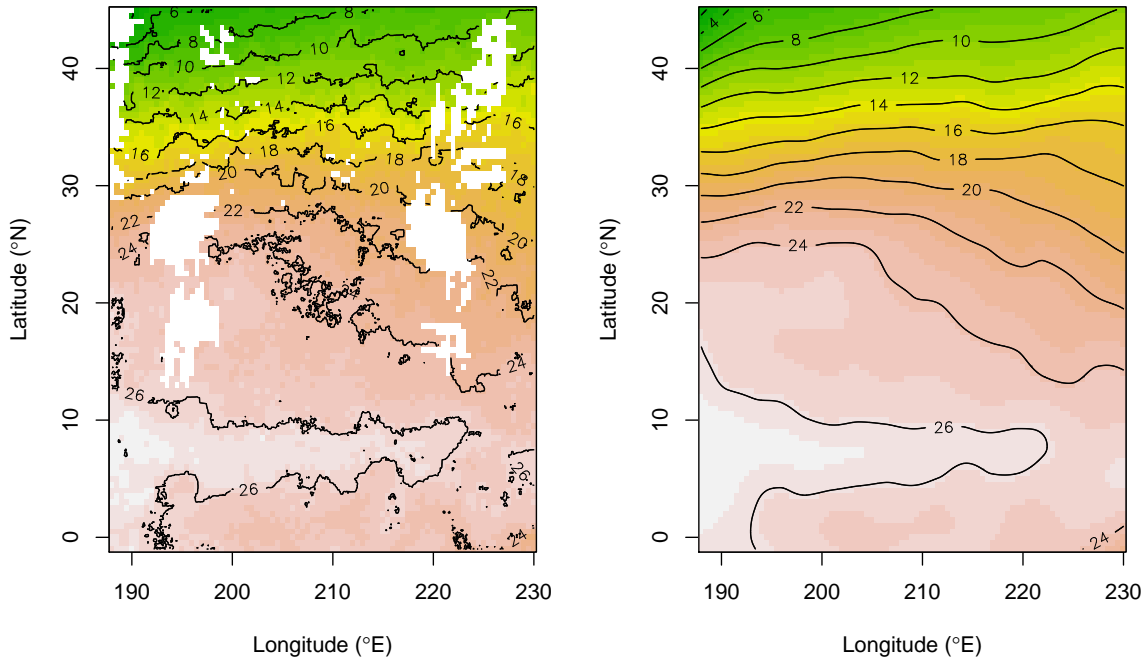
7

Figure 1: The observed fine-scale SST field from the first week of January 2001 (left), and the (5% nearest neighbor fraction) smoothed version used by Kalman filter (right).

For the purposes of the Kalman filter, the estimated SST field is represented by a local polynomial regression (Loader 1999). This algorithm fits local polynomials to the observations to ensure a surface smoothed to a degree specified by the modeler. The 'nearest neighbor fraction' determines what fraction of the nearest points are used to fit the local polynomial. For the tracks analyzed here, a nearest neighbor fraction of 5% was chosen. Three different degrees of smoothing were tested (2.5%, 5%, 10%) to investigate the sensitivity to the degree of smoothing. Advantages of this algorithm are that data can be smoothed to the extent necessary, the derivative field is computed directly by the smoothing algorithm, and predictions can be made where data are missing. Figure 1 shows an example of a smoothed SST field.

The most probable track

The Kalman filter and the maximum likelihood principle supply estimates of the model parameters and the predicted track. A point on the predicted track at any given time point is calculated using all observations available at that time; $\widehat{\alpha}_i = E(\alpha_i|y_1,\ldots,y_i)$. Better estimates can be produced once the entire track is known. The most probable track is calculated using all observations after all parameters have been estimated; $\widehat{\alpha}_{i|T} = E(\alpha_i|y_1,\ldots,y_T)$.

The actual computation of the most probable track is done in a single backwards updating sweep of the predicted track. The last point of the most probable track is identical to the last point of the predicted track, as all observations were available to the predicted track at the final point. The last point of the most probable track is known $\widehat{\alpha}_{T|T} = \widehat{\alpha}_T$ and the prediction error of the last point $P_{T|T} = P_T$. The following equations are used to compute the previous points of the most probable track.

(15) $\quad \widehat{\alpha}_{i|T} = \widehat{\alpha}_i + P_i^{\star} \left(\widehat{\alpha}_{i+1|T} - \widehat{\alpha}_i - c_{i+1} \right) \qquad$ update position given all observations

(16) $\quad P_{i|T} = P_i + P_i^{\star} \left(P_{i+1|T} - P_{i+1|i} \right) P_i^{\star\prime} , \quad \text{where} \quad P_i^{\star} = P_i P_{i+1|i}^{-1}$

This technique is known as "smoothing" in textbooks on the Kalman filter (e. g. Harvey 1990), as the resulting track most often is smoother than the predicted track. The matrix $P_{i|T}$ is the covariance estimate of the i'th position estimate on the most probable track measured in nautical miles. $P_{i|T}$ is a measure of the variability of the position estimate after all observations (past and future) have been taken into account.

Fixed pop-up position

If the last position is known without error, or with an error term which is negligible compared to the light-based geolocations, it can be used as a fixed point. This corresponds to setting the measurement error and the measurement bias to zero for the last observation ($(H_T)_{1,1}$, $(H_T)_{2,2}$, $(d_T)_1$, and $(d_T)_2$ all zero). This results in a predicted (and most probable) track ending up in the fixed pop-up location.

RESULTS

The tags on both drifters tags reported on schedule. PAT 21760 should have transmitted 6024 readings for both depth and temperature. For the raw depth histogram data, only 107 readings were received (1.8% of all possible readings). For the raw temperature histogram data, only 96 readings were received (1.6% of all possible readings). For the profile of depth-temperature data (PDT), only 92 readings were received (1.5% of all possible readings). From the PDT data the average of the daily SST temperature readings at the surface were taken. Software from the manufacturer (dated March 2003) was used to estimate geolocations for the PSAT and 167 estimates were given (66.5% of all possible days). As a comparison, the GPS drifter buoy over the same time period transmitted 7316 geolocations (more than one per hour) and 1166 SSTs (or 19.4%).

PAT 21765 should have transmitted 5856 readings for both depth and temperature. For the raw depth histogram data, only 81 readings were received (1.4% of all possible readings). For the raw temperature histogram data, only 71 readings were received (1.2% of all possible readings). For the profile of depth-temperature data (PDT), only 92 readings were received (1.6% of all possible readings). Software from the manufacturer was used to estimate geolocations for the PSAT and 154 estimates were given (63% of all possible days). As a comparison, the GPS drifter buoy over the same time period transmitted 7,521 geolocations (more than one per hour) and 1,234 SSTs (or 21.1%).

The shark affixed with PSAT 13093 spent 90% of it's depth at 100m or less. Shark with tag 13097 spent 90% of it's time at 160m or less and had a high correlation between average nighttime depth and lunar illumination indicating a pronounced diel depth pattern. For PSAT 13097, at liberty for 233 days 47% of the possible raw depth and temperature data and 42% of geolocations were received. For PSAT 13097, at liberty for 102 days 50% of the possible raw depth and temperature data and 42% of geolocations were received.

Analysis of the two tagged female blue sharks with the method using only the light-based geolocations, and the extended method with SST showed pronounced differences in the estimated most probable tracks (Fig. 2 and Fig. 3). The longitude estimates for the most probable tracks remained fairly unchanged by the inclusion SST. The latitude estimates of the most probable tracks were dramatically changed by inclusion of SST (Fig. 2 and Fig. 3). These results are not surprising since longitudinal SST gradients are small while latitudinal SST gradients are large in this region. The
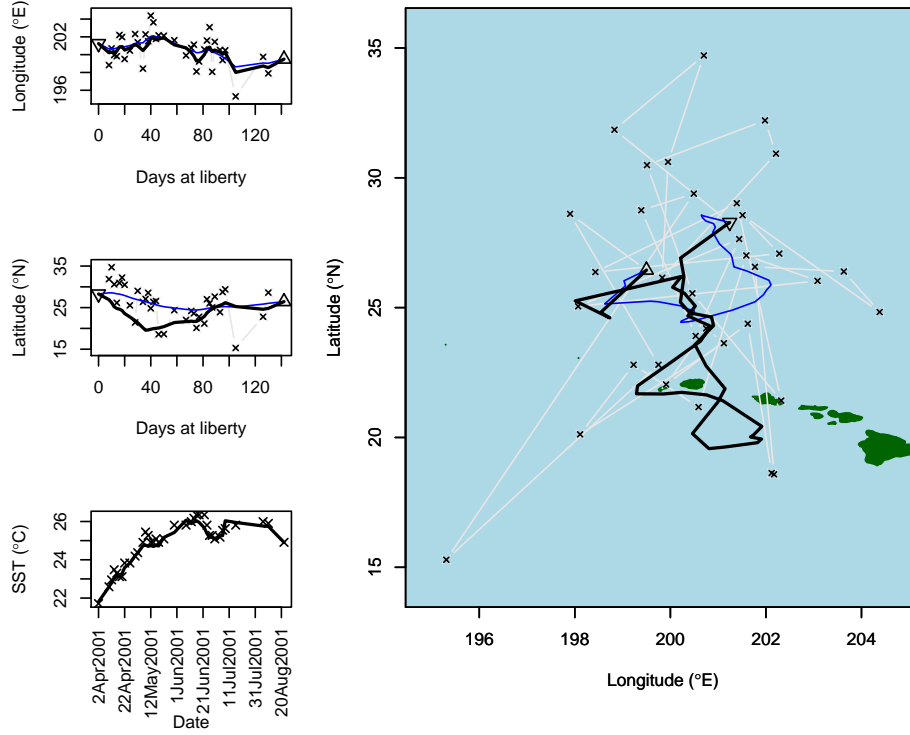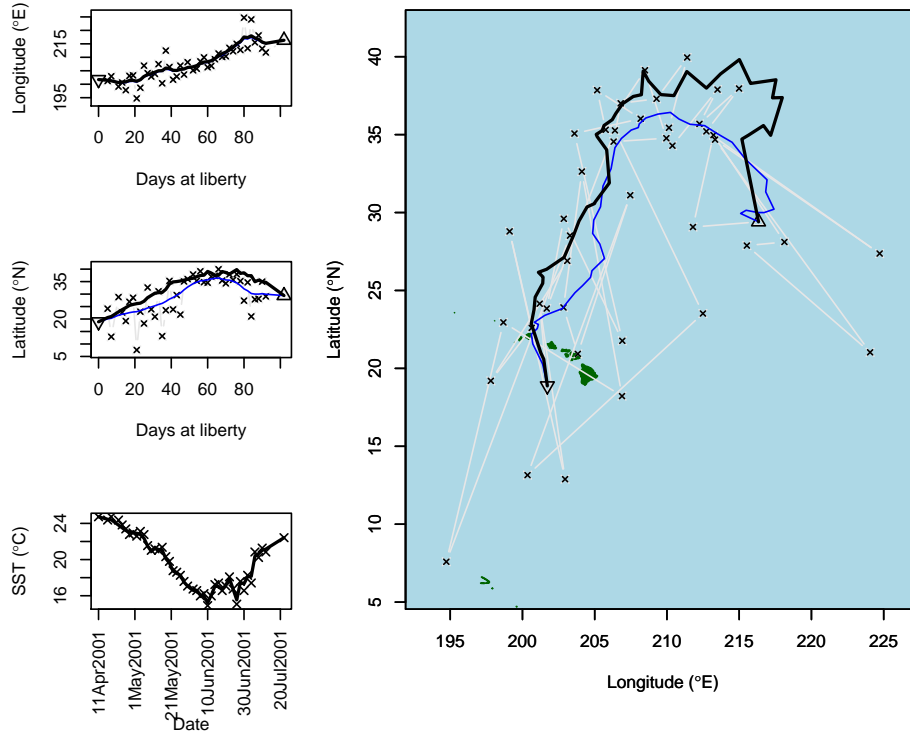
Figure 2: Most probable track for blue shark number 13097 (right) fitted with (thick line) and without SST information (thin line). Thin white line connects the raw light-based geolocations. Left panel shows how well the model fits the three different information sources (longitude, latitude, and SST). Raw geolocations and observed SST are marked by crosses, deployment point is marked by '▽', and known recapture/pop-up position is marked by '△'.

variation of the latitude observations (second plot in left panel) around the most probable track is much larger than the variation of the tags SST measurements compared to the remotely sensed SSTs along the most probable track (third plot left panel).

To quantify the difference between tracks estimated with and without SST measurements, the covariance of each point on the most probable track was calculated from the covariance matrix $P_{i|T}$ in (16). The resulting covariance for each point along the track matrix is transformed into degrees of longitude and latitude by the delta method, $V_i = \widehat{Z}_i P_{i|T} \widehat{Z}'$. V_i is now an estimate of the covariance of the i'th point on the

Figure 3: Most probable track for for blue shark number 13093 (right) fitted with (thick line) and without SST information (thin line). Thin white line connects the raw light-based geolocations. Left panel shows how well the model fits the three different information sources (longitude, latitude, and SST). Raw geolocations and observed SST are marked by crosses, deployment point is marked by '▽', and known pop-up position is marked by '△'.

most probable track expressed in degrees of longitude and latitude. This variance could for instance be used to construct confidence intervals (ellipses) for each point on the track.

The longitude variance $(V_i)_{1,1}$ of both tracks was not changed much by including SST. This was expected, as the SST field is fairly constant longitudinally. For track number 13097 the latitude variance $(V_i)_{2,2}$ was also very similar. The average latitude variance with SST was 0.73 compared to 0.75 without SST. This was slightly surprising. A closer look revealed that this blue shark was swimming at latitudes where the temper-
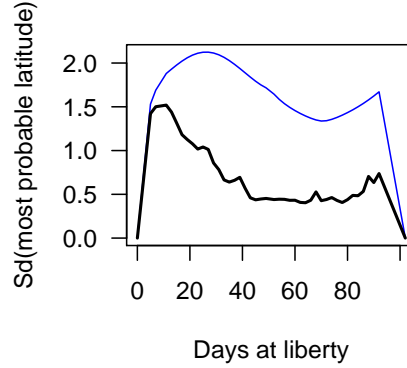
12

Figure 4: Estimated standard deviation for the latitude component of the most probable track 13093 estimated with (lower thick line) and without SST information (upper thin line).

ature gradient was not very steep (compare Fig. 2 to Fig. 1). For track number 13093, the latitude variances were much lower when SST measurements were included. The average latitude variance with SST was 0.59 compared to 2.9 without SST. The latitude standard deviation for each point on the most probable track estimated with and without SST measurements (Fig. 4) illustrates the difference. The latitude standard error of the purely light-based method is between 1.5 and 2 degrees, meaning that a 95% confidence interval could span up to 8 degrees. The standard error of the method including SST is between 0.4 and 1.5, and about half of the time around 0.5, which corresponds to a 95% confidence interval spanning only 2 degrees. The average longitude variance was 2.3 for track number 13093 and and 0.54 for track number 13097 both estimated in the model with SST.

The double-tagging buoy experiment was not designed to evaluate the method of incorporating SST, but to investigate the error structure of light-based geolocations. Unfortunately the light-based latitude information from these specific tags produced estimates with huge geolocation errors (Fig. 5 and Fig. 6). With measurement errors of up to 50 degrees latitude, this information is practically useless. However, the double-tagging buoy experiment offers a unique opportunity to test the SST method in the absence of consistent latitude information on a moving tag.
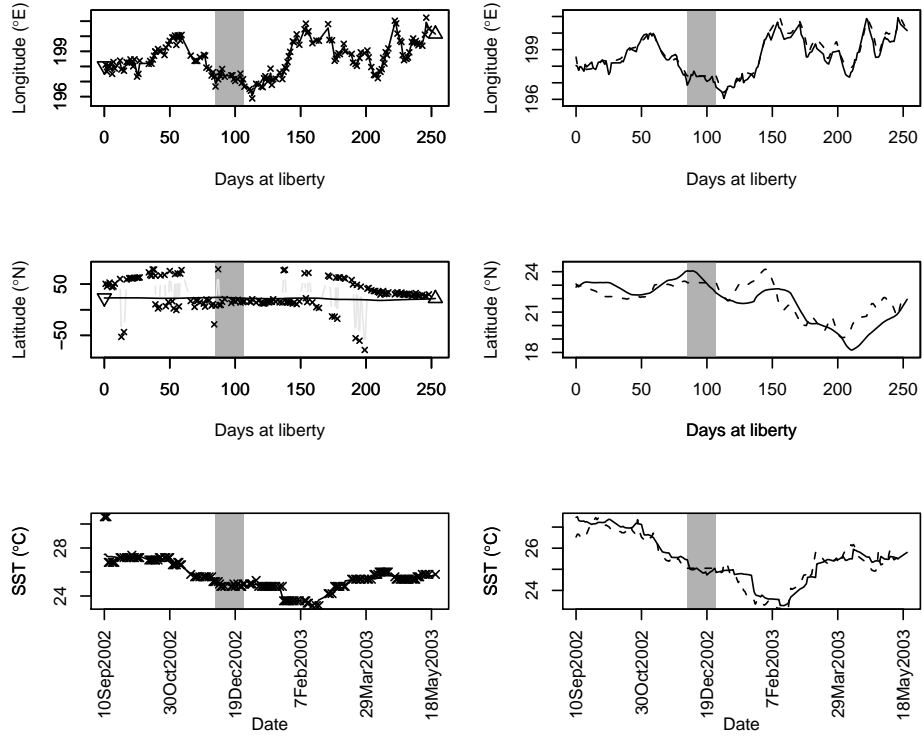
Figure 5: Most probable track for drifter buoy 21760 (solid line) compared to the raw observations (crosses left plot), and to the true positions from GPS measurements (dashed lines right plot). The shaded area indicates a time period when the buoy was beached on an island.

The first double-tagging buoy experiment (Fig. 5) showed that the SST-enhanced method is able to estimate the actual track of the drifter buoy. The estimated longitude coordinates from the most probable track match the GPS-determined longitude very closely as expected (the root mean squared, or rms, difference=0.31 degrees) and are slightly better than the raw longitude (rms difference=0.36). The latitude coordinates are also close to the GPS-determined latitude (rms difference=0.99 degrees), which is more remarkable, as the raw latitude was not very helpful (rms=29.23 degrees). The most probable latitude track is derived almost solely from SST information. The buoy beached itself for a period of three weeks and then went back into the water (Fig. 5). The buoy kept transmitting and recording, and the reconstructed track seems unaffected by stranding.
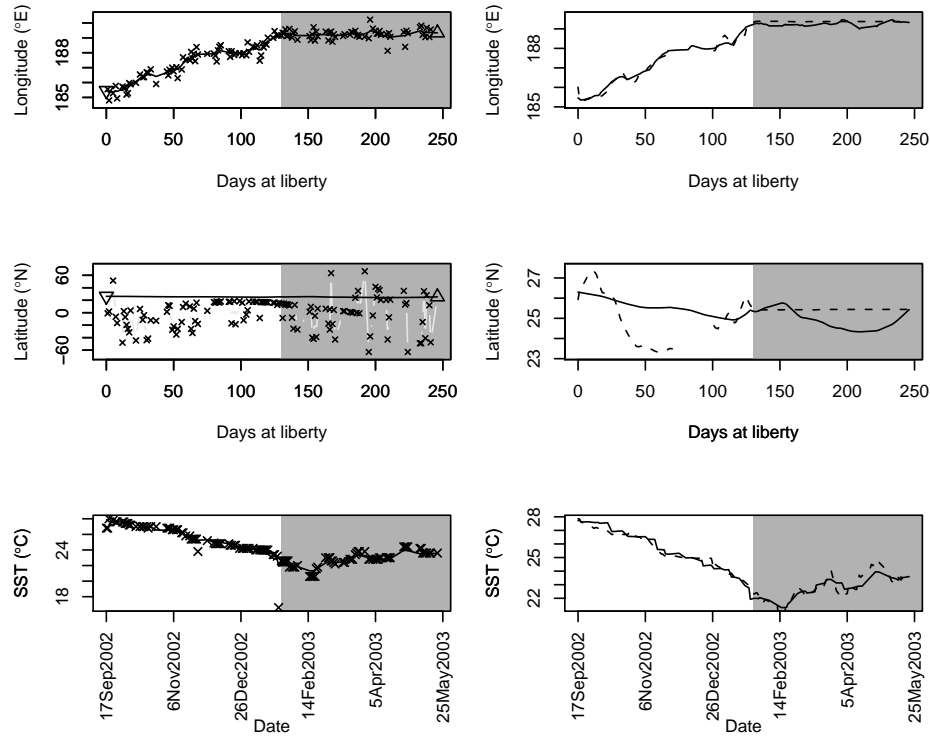
14

Figure 6: Most probable track for drifter buoy 21765 (solid line) compared to the raw observations (crosses left plot), and to the true positions from GPS measurements (dashed lines right plot). The shaded area indicates a time period when the buoy was caught on a reef.

The second double-tagging buoy experiment (Fig. 6) is more problematic to evaluate, as the buoy was caught in a reef about half of the time. The most probable longitude track agrees well with the GPS information (rms difference=0.15) and is better than the raw longitude estimates (rms difference=0.32). Raw latitude measurements had errors up to 60 degrees (rms difference=36.17) compared to the actual track. The most probable latitude track is off by only one or two degrees from the actual track and had smaller rms differences (1.00). The buoy entered Maro Reef after 120 days at liberty and remained within the reef complex for the last four months (Fig. 6). The PSAT functioned normally during this period recording data and transmitting on schedule.

15

To illustrate the sensitivity of the degree of smoothing to the SST temperature field, three different degrees of smoothing were tested on the four tracks. Normal (5% nearest neighbor fraction), twice as coarse (10%), and twice as fine (2.5%). Here fine refers to less smoothing, which is closer to the observed SST field. This sensitivity analysis showed only minor differences between the reconstructed tracks (Fig. 7). In fact, most of the tracks were identical. In one case, the very finest smoothing seemed to give a more variable track in a few points.
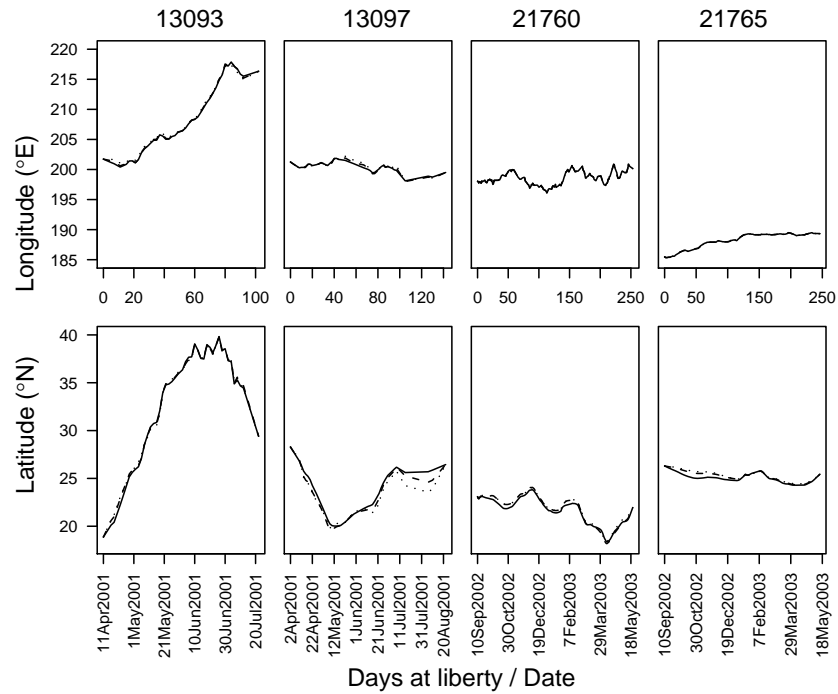

Figure 7: Most probable longitude (top row) and latitude (bottom row) of the four estimated tracks with three levels of smoothing of the SST field. normal (dashed line), twice as coarse (solid line), and twice as fine (dotted line). Fine-scale SST fields were applied to tracks 13093 and 13097. Mesoscale data were applied to tracks 21760 and 21765.

The degree of smoothing used in the track analysis was chosen simply by looking at the smoothed fields compared to the observed fields. A more objective and automatic approach would be to select the degree of smoothing based on a cross-validation scheme (Efron and Tibshirani 1993).

16

DISCUSSION

Geolocation based on indirect measurements is unlikely to ever achieve the precision of GPS methods, but combining several indirect measurements in a coherent manner is the best solution possible. The latitude variance estimates, $(V_i)_{2,2}$, and substantially lower that those anticipated by Smith and Goodman (1986) and approach the theoretical limit discussed by Metcalfe (2001).

The general approach of matching individual measurements to a corresponding externally determined field, within the milieu of the Kalman filter, can potentially be used to further improve (or replace) light-based geolocation by including more measurable or detectable environmental variables. For instance salinity, geomagnetism, chemical tracers, or water depth for demersal species (Hunter et al. 2003). The present paper demonstrates the use of supplementary fields by illustrating how the inclusion of SST measurements is able to reduce the geolocation error substantially (Fig. 4), and even reconstruct a track where the light-based latitude measurements were practically useless (Fig. 5). Reduction in geolocation error is greatest in the directions and areas where the gradient of the ancillary field is steepest. In the case of SST, the SST field in the study area had steepest gradients in the latitude direction, which is also the direction where light-based geolocation is poorest. When considering to include additional variables to improve geolocation, it should be a concern weather or not that information is really already implicitly represented. For instance, if the SST field and the salinity field are proportional in the study area, it would not contribute much to include them both. The state space Kalman filter approach (Sibert et al. 2003) is an important part of the presented method. It ensures that the matching between tag observations and the underlying field is done locally. The field can potentially have many areas where the value matches the tag observed value, and the Kalman filter provides an objective method to select the value that is most consistent with all observations.

Drifter buoys are not the perfect tools for evaluating how well this method works on live animals, as their behavior is somewhat different. Free-ranging large pelagic fish make vertical excursions in the water column, and tend not to run aground on a beach for three weeks. These abnormal periods could have influenced the SST measurements. The three week beaching seems not to have influenced the measurements or the reconstructed track. The four months at a fixed position in the shallow waters of a reef might have given slightly higher SST readings than if a tagged individual was swimming freely in the surrounding waters. This may account for the more southerly estimated track. Despite these difficulties the drifter buoy experiments demonstrate

that SST is very useful in estimating latitude, even when the light-based latitude is practically useless.

The inclusion of ocean temperature in the Kalman filter estimation process could result in more accurate geolocations for several pelagic species. Light based geolocations are problematic for species with large diurnal vertical migrations (e.g. swordfish, bigeye tuna and thresher sharks). These species descend before dawn to occupy mesopelagic depths during the day and ascend after dusk to occupy near-surface depths at night. Latitude estimates are often inaccurate due to dim ambient light at mesopelagic depths and extensive vertical movements at the time of dawn and dusk (Musyl et al. 2001). However, these species often occupy the mixed layer during the night and SST information could improve the geolocations. Takahashi *et. al* (2003) used a searching algorithm to match tag temperatures at 0, 80 and 160 m to ocean temperatures at a monthly $2°$ latitude and $5°$ longitude scale to estimate latitudes from an archival tag recovered from a swordfish. A similar approach could be envisaged in a Kalman filter process whereby tag temperatures at several depths could be linked with observed temperature-at-depth data or OGCM model output.

A simple sensitivity analysis was conducted to illustrate the effect of smoothing the SST temperature field. While current results indicate only minor differences when using three different degrees of smoothing, further work is required to investigate the spatial as well as temporal effects of scale and smoothing. The appropriate scale of SST data and smoothing will depend on several factors such as the ocean dynamics in the study area and data quality due to cloud cover. Scale and smoothing considerations would be different for an analysis of a western boundary current (Kuroshio, Gulf Stream) region compared to a less stratified mid-ocean gyre. The abundance of clouds may dictate the scale and smoothing required as the Kalman filter requires that all points be included in the study area and smoothing was necessary to remove SST pixels with no data (excessive cloud cover), especially in the fine-scale (9 km) data.

It is important to mention, that using the average of the water temperature measurements collected from the tag at depths less than 15 meters is an arbitrary choice. Using for instance the median or the mode might work equally well (or better) within the framework of the outlined method. Similarly, other sources and scales of SST fields should be considered.

The application of SST to estimation of positions from archival tag data inevitably requires some arbitrary decisions: a specific SST product, scale and resolution must be selected; a means to estimate SST from data recorded by the tag must be devised; a

criterion to determine what constitutes a match between environmental and tag SST estimates must be specified. Modifications to the Kalman filter model described here eliminate the third decision by including the SST variance in the likelihood function (14) in a statistically consistent way with other sources of variance. Furthermore, smoothing the SST surface and the use of averaging to compute the tag SST mitigate the consequences of the first two decisions. Other temperature correction methods assume that the light-based longitude estimates are either error-free or have errors that can be reduced to near zero by removal of outliers. The Kalman filter makes no such assumptions and uses all of the data. In principal, inclusion of SST also enables correction of longitude errors where tracks cross regions with large longitudinal SST gradients.

ACKNOWLEDGEMENTS

REFERENCES

Arnold, G., and Dewar, H. (2001) Electronic tags in marine fisheries research: a 30-year perspective. In: *Electronic Tagging and Tracking in Marine Fisheries Reviews: Methods and Technologies in Fish Biology and Fisheries.* J.R. Sibert & J.L. Nielsen (eds) Dordrecht: Kluwer Academic Press, pp. 7–64.

Efron, B., and Tibshirani, R. J. (1993) *An Introduction to the Bootstrap*. Chapman & Hall.

Gunn, J., and Block, B. (2001) Advances in acoustic, archival, and satellite tagging of tunas. In: *Tuna Physiology, Ecology, and Evolution.* B.A. Block & E.D. Stevens (eds) NY: Academic Press, pp. 167–224.

Gunn, J., Polachek, T., Davis, T., Sherlock, M., and Betlehem, A. (1994) The development and use of archival tags for studying the migration, behaviour and physiology of bluefin tuna, with an assessment of the potential for transfer of the technology for groundfish research. *ICES C.M. Mini,* **21**.

Harvey, A. C. (1990) *Forecasting, Structural Time Series Models and the Kalman Filter*. Cambridge University Press, Cambridge.

Hill, R. (1994) Theory of geolocation by light levels. In: *Elephant Seals: Population Ecology, Behaviour, and Physiology.* LeBoeuf, B. J. and Laws, R. M. (eds) University of California Press, Berkeley, CA, pp. 227–236.

Hill, R. D., and Braun, M. J. 2001. Geolocation by Light Level - The Next Step: Latitude. *In* J.R. Sibert and J. Nielsen (Eds.), Electronic Tagging and Tracking in Marine Fisheries (pp. 315-330). Kluwer Academic Publishers, The Netherlands.

Hunter E., Aldridge, J. N., Metcalfe, J. D., Arnold, G. P. (2003) Geolocation of free-ranging fish on the European continental shelf as determined from environmental variables: I. Tidal location method. *Marine Biology* **142**:601–609.

Inagake, D., Yanada, H., Segawa, K., Okazaki, M., Nitta, A., and Itoh, T. (2001) Migration of young Bluefin Tuna, *Thunnus orientalis* Temminck et Schlegal, through archival tagging experiments and its relation with oceanographic conditions in the western North Pacific. *Bull. Nat. Res. Inst. Far Seas Fish.* **38**:53–81.

Jonsen, I. D., Myers, R. A., and Flemming, J. M. (2003) Meta-analysis of animal movement using state-space models. *Ecology* **84**: 3055-3063.

Kalman, R. E. (1960) A New Approach to Linear Filtering and Prediction Problems. *Transactions of the ASME–Journal of Basic Engineering* **82**:35-45

Loader, C. (1999) *Local Regression and Likelihood*. Springer, New York.

Metcalfe, J. D. (2001) Summary report of a workshop on daylight measurements for geolocation in animal telemetry. In: *Electronic Tagging and Tracking In Marine Fisheries Reviews: Methods and Technologies in Fish Biology and Fisheries,* J. Sibert and J. Nielsen (eds.) Dordrecht: Kluwer Academic Press, pp. 443-456.

Musyl, M. K., Brill, R. W., Curran, D. S., Gunn, J. S., Hartog, J. R., Hill, R. D., Welch, D. W., Eveson, J. P., Boggs, C. H., and Brainard, R.E. (2001) Ability of archival

tags to provide estimates of geographical position based on light intensity. In: *Electronic Tagging and Tracking in Marine Fisheries Reviews: Methods and Technologies in Fish Biology and Fisheries.* J.R. Sibert & J.L. Nielsen (eds) Dordrecht: Kluwer Academic Press, pp. 343–368.

Musyl, M. K., Brill, R. W., Boggs, C. H., Curran, D. S., Kazama, T. K., Seki, M. P. (2003) Vertical movements of bigeye tuna (*Thunnus obesus*) associated with islands, buoys, and seamounts near the main Hawaiian Islands from archival tagging data. *Fish. Oceanogr.* **12**:152–169.

Reynolds, R. W., and Smith, T. M. (1994) Improved global sea surface temperature analyses using optimal interpolation. *J. Climate* **7**:929–948.

Sibert, J., Musyl, M. K., and Brill, R. W. (2003) Horizontal movements of bigeye tuna (*Thunnus obesus*) near Hawaii determined by Kalman filter analysis of archival tagging data. *Fish. Oceanogr.* **12**:141–151.

Smith, P., and Goodman, D. (1986). Determining fish movement from an 'archival' tag: precision of geographical positions made from a time series of swimming temperature and depth. *NOAA Technical Memorandum, NOAA-TM-NMFS-SWFC-***60** *13pp.*

Takahashi, M., Okamura, H., Yokawa, K., and Okazaki,M. 2003. Swimming behaviour and migration of a swordfish recorded by an archival tag. *Mar. Freshwater Res.* **54**:527-53.

Teo, S. L. H., Boustany, A., Blackwell, S., Walli, A., Weng, K. C., Block, B. A. (2004) Validation of geolocation estimates based on light level and sea surface temperature from electronic tags. *Mar. Ecol. Prog. Ser.* **283**:81–98.

Vazquez, J., Perry, K., and Kilpatrick, K. (1998) NOAA/NASA AVHRR Oceans Pathfinder Sea Surface Temperature Data Set User's Reference Manual Version 4.0. 10 April 1998, JPL Publication D-14070.

Wilson, R. P., Ducamp, J. -J., Rees, W. G., Culik, B. M., and Neikamp, K. (1992) Estimation of location: global coverage using light intensity. In: *Wildlife Telemetry: Remote Monitoring and Tracking of Animals.* Ellis Horwood, NY, pp 131–134.

Wilson, S. G., Lutcavage, M. E., Brill, R. W., Genovese, M. P., Cooper, A. B., Everly. A.W. (2005) Movements of bluefin tuna (Thunnus thynnus) in the northwestern Atlantic Ocean recorded by pop-up satellite archival tags. *Marine Biology* **146**:409–423.